

# Origin of Cylindrically Oriented Zonal Flows in the Jovian Planets as Dictated by Quantum Celestial Mechanics (QCM)

Franklin Potter

Sciencegems, 8642 Marvale Drive, Huntington Beach, CA, 92646, USA. E-mail: frank11hb@yahoo.com

The four Jovian planets in the Solar System have fluid bodies surrounding a solid core and each exhibit several complex zonal flows with their atmospheres moving faster than the planet rotation. Several research groups have proposed that these atmospheric east-west zonal jet flows that are aligned with the axis of rotation are cylindrically confined, as indicated by identifying gravity harmonics. I propose that the source of these co-axial concentric cylindrical flow zones is dictated by quantum celestial mechanics (QCM), which states that the equilibrium radius for each cylindrical band/zone within the planet occurs where the Newtonian gravitational attraction balances the repulsive QCM quantization of angular momentum per unit mass effect.

## 1 Introduction

The four Jovian planets in our Solar System are fluid bodies surrounding a solid core. Fluid bodies do not rotate as rigid bodies and, instead, exhibit complex zonal flows in the atmospheres. Observational evidence of the Jovian planets by spacecraft in the visible, the ultraviolet (UV), the infrared (IR), and with magnetic field sensing, reveals atmospheric east-west zonal jet flows in each hemisphere. For a review that includes detailed diagrams of these zonal flows in the atmosphere down to a few thousand kilometers for Jupiter and Saturn, see [1].

These bands/zones on Jupiter have been observed through optical devices since the 1600s, but only via using data collected by the Juno and Cassini orbiting spacecraft at Jupiter and Saturn have researchers significantly improved our description of this complex zonal flow behavior.

Detailed analyses identifying gravity harmonics by several research groups over the past decade and earlier have suggested that the Jupiter and Saturn flows are probably aligned with the axis of rotation and that cylindrical confinement is essential for each distinct observed dynamic flow behavior. Specifically, as one example, in Jupiter the  $21^\circ$  N jet provides evidence that the flows extend inward cylindrically and not much radially [2]. For the equivalent cylindrical flow behavior on Saturn, see [3].

For all four Jovian planets, the flows penetrate cylindrically downward, to a depth of about 3000 km in Jupiter, to about 9000 km in Saturn, and to about 1000 km in Uranus and in Neptune. More than one cylindrical flow region exists within each Jovian planet. As a very simplified suggestion of the geometry being considered, Fig. 1 shows how two possible co-axial concentric flow cylinders would penetrate throughout a planetary sphere.

As these cylindrical regions rotate faster than the planet rotation, there would be physical flow phenomena to be measured along the concentric circular regions where each cylinder pierces the surface. One should note that there would be

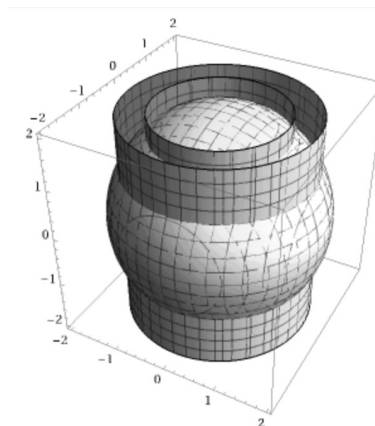


Fig. 1: Two co-axial concentric QCM cylinders penetrating the planet.

overlap among the cylindrical regions at most depths because they each could have a radial thickness that increases with depth within the planet.

The actual physics origin of such cylindrical regions for the atmospheric flows within these Jovian planets has not been identified. Some complex suggestions involving dynamical combinations of Coriolis effects, temperature gradients, pressure gradients, magnetic field influences, etc., have been incorporated into existing models, but there has been no definitive single source proposed for the cylindrical symmetries [4, 5].

I propose that these co-axial concentric cylindrical flow zones can exist within all planets because they are dictated by the gravitational forces resulting from the quantization of angular momentum per unit mass constraint of quantum celestial mechanics (QCM) [6]. Equilibrium radii for the concentric cylinders within a massive body such as a planet are determined by both Newtonian gravitational attraction and a quantization of angular momentum per unit mass repulsive effect.

The equilibrium orbital radii of the planets of the So-

lar System as well as the orbital distances for planets in all known multi-planetary exosystems have been shown to obey this angular momentum constraint dictated by QCM in the Schwarzschild metric environment. Because each planet has a Schwarzschild radius  $r_s$  of a few meters or less, this quantization of angular momentum per unit mass effect applies also within the planets with the result being co-axial concentric cylindrical rotating regions.

## 2 Some prior applications of QCM

For an abbreviated derivation of quantum celestial mechanics (QCM) from the general relativistic Hamilton-Jacobi equation and some of its equations predicting gravitational effects for bodies obeying the Schwarzschild metric, see the Appendix. Applications of QCM in other gravitational metrics can be found in the original paper [6] and in several other of the references [7–11].

We have used QCM to explain the spacings of planetary orbits in the Solar System and in all known exoplanetary systems [8]. Essentially, QCM predicts both the Newtonian gravitational attraction and a repulsive effect [see (10) in the Appendix] that together specify equilibrium orbital radii that are a small subset of all possible Newtonian equilibrium orbital radii.

All known multi-planetary exosystems have been shown to obey this angular momentum constraint dictated by QCM. In the Solar System, we learned that the Oort Cloud, with its angular momentum contribution being almost 50 times greater than the angular momentum contributions of the planets plus the Sun, dictates the allowed equilibrium orbital radii of the planets to explain why its large radial separations are unique among the known planetary systems. Fig. 2 shows a sample of these exosystems obeying the angular momentum constraint. Note that they have planets closer to their star than the orbit radius of Mercury, and in some cases, they have a Jupiter mass planet close-in!

After applying the gravitational wave equation (GWE) in the Schwarzschild metric to planetary systems [8], we found further applications to galaxies, clusters of galaxies [9], and to the Universe. For the Universe [10], we determined an alternate viable explanation of cosmological redshifts in a static Universe in the interior metric, i.e. that a non-linear negative gravitational potential exists that agrees with the SN1a data for an accelerating behavior. Our result suggests that the clocks at the distant light sources tick slower than clocks at the observer for all observers.

For the analysis of the Jovian planets, we will use the same quantization of angular momentum per unit mass constraint dictated by QCM for the Schwarzschild metric given by (8) in the Appendix, which becomes

$$L/\mu = m L_T/M_T \quad (1)$$

for integer  $m$  and a gravitationally bound system total angular momentum  $L_T$  and total mass  $M_T$ .

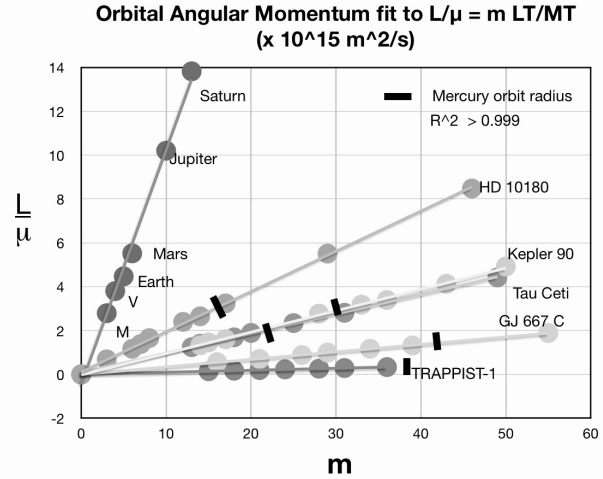


Fig. 2: The QCM angular momentum per unit mass constraint applied to several multi-planetary exosystems. The short line marks the orbital radius distance of Mercury. The slopes are proportional to the total angular momentum in the gravitationally bound systems.

The application of this QCM orbital quantization equation is not only for planets in the exterior space surrounding the central massive object of mass  $M$  but also for the interior volume within the mass for all equilibrium radii  $r_{eq}$  greater than the Schwarzschild radius  $r_s > 2GM/c^2$ .

In 2021, we investigated radial distances from the Earth's axis within the Earth itself to establish [11] that the Antarctic Circumpolar Current (ACC), a significant water current moving eastward completely around the Antarctic Continent about 2 meters/second faster than the Earth's rotation at its latitude, exists at the  $m = 6$  radial distance and is probably being driven by our QCM effect. That is, the ACC lies at the Earth's surface where a QCM rotational co-axial cylinder parallel to the Earth's axis penetrates the surface from the interior. Normally, one would expect a similar eastward water current around the North Pole region at about the same North latitude as the ACC, but land masses block such a continuous water current.

Recent seismic research [12] has revealed also that deep within the Earth, within its fluid outer core, lies a large donut-shaped mass, i.e. a toroidal volume, that rotates independently about the Earth's rotation axis at a different angular velocity than the rest of the outer core. Located at nearly the same radial distance from the Earth's axis as the ACC, we are investigating whether this rotating donut could be driven by the QCM gravitational force produced by the same cylinder with  $m = 6$  as for the ACC.

## 3 Jovian planet considerations

In this investigation we are analyzing much more complicated dynamic systems involving planets with significant gaseous atmospheres. We consider whether the rotational zone/band structures of the Jovian planets, Jupiter, Saturn, Uranus, and

Neptune, are produced by the above QCM angular momentum constraint equations. Their Schwarzschild radii are all less than 3 meters, so they are expected to have rotational cylindrical regions co-axially parallel to the planet's rotation axis within their massive bodies.

However, unlike the Earth that is essentially dense solid and liquid matter all the way to its total radius, the Jovian planets each possess a fluid atmosphere that is a mixture of gases that extends significantly into the planet from the “surface”, which is defined to be where the pressure is 1 bar. This atmospheric difference down to thousands of meters complicates any analysis.

Fortunately, the combined effects of Coriolis forces, temperature gradients, magnetic field movement, etc., have been worked out in terms of Bessel functions and Legendre functions [1–3] for the geometry of the dynamic flows within the band structures. What is absent, however, is the reason for the existence of the proposed rotating co-axial concentric cylindrical regions within the rotating planets.

We will determine possible radii for the QCM co-axial concentric cylinders from the angular momentum constraint given by (1) based upon the physical parameters at each Jovian planet and try to determine whether they are the source of the cylindrical geometries for the atmospheric bands existing at the “surface”. That is, if the radii of the predicted cylindrical regions roughly agree with the radii of the atmospheric zones/bands, we will consider that we have identified their source. In order to simplify our derivation of the cylindrical symmetry behavior within these planets, we will assume a north-south symmetry approximation for these band/zone regions, although there exists an obvious asymmetry in the flow data when the northern and southern hemispheres are compared.

Fig. 1 shows an example of only two co-axial concentric cylinders for a spherical planet. Where each cylinder intersects the “surface” is where the bands/zones should be. Because each cylinder has some width in the radial direction, the widths of each cylinder can overlap more than one other cylinder beneath the surface inside each planet, thereby creating a more complex environment than we will investigate. These complexities are probably already incorporated into the research models mentioned above.

#### 4 Jovian planet analysis

If the planets were solid, their effective planet radii would be easy to define. However, a planet such as Jupiter has a solid core plus a liquid outer core region plus a significant lower density additional atmospheric region. One needs to determine the effective radius  $R$  of the planet for the application of the quantization of angular momentum per unit mass constraint in (1), which cannot be the radius  $R_0$  to the “surface” because the atmosphere that occupies the outer radius is itself being driven by the QCM effective force determined by the

Table 1: Effective planet radius for the Jovian planets.

Planet	$\alpha$	$\alpha R^2$ ( $\times 10^{14} \text{m}^2$ )	$R$ ( $\times 10^7 \text{m}$ )	Ratio $R/R_0$
Jupiter	0.2756	3.0	3.26	0.455
Saturn	0.22	4.0	4.26	0.71
Uranus	0.33	1.5	2.55	1.0
Neptune	0.33	1.4	2.46	1.0

dense inner regions.

Applying (1), we substitute  $vr$  for  $L/\mu$  on the left side, with  $v$  being the tangential velocity of mass  $\mu$  at orbit radius  $r$ , and substitute  $\alpha MR^2 \omega/M$  for  $L_T/M_T$  on the right side, to obtain the equilibrium radius expression

$$r_{eq}^2 = m \alpha R^2, \quad (2)$$

where  $\alpha$  is the moment of inertia coefficient, i.e. of  $\alpha MR^2$ , and  $R$  being the effective radius. For a solid planet,  $R$  would be the radial distance  $R_0$  to its physical surface, but for the fluid Jovian planets,  $R$  may not be this distance.

We define an effective radius  $R$  to be the one that produces the correct latitudinal distribution of bands/zones at the surface of the planet. The effective  $\alpha MR^2$  values for the four Jovian planets are listed in Table 1. Note that for both Jupiter and Saturn, the effective radius  $R$  is much less than the actual radius  $R_0$  of the planet as revealed in the ratio column, whereas for Uranus and Neptune the effective radius is probably the total radius of the planet. Also recall that for both Uranus and Neptune, the actual zonal latitudinal structures have not been identified as well as achieved for Jupiter and Saturn. Hopefully, more information will become available in the near future to ascertain whether our results actually agree with their band/zone structures.

The effective radius values in Table 1 are used to determine the  $r_{eq}$  values predicted by (1) and their equivalent latitudes for comparison to the data. The calculated values for the QCM co-axial concentric cylinders within the planets as listed in Table 2 for Jupiter and Saturn and in Table 3 for Uranus and Neptune.

The predicted latitudes for the zones/bands are in reasonable agreement with those at the surfaces of Jupiter and Saturn, but we await further data for the zone/band data for Uranus and Neptune.

Jupiter's differential rotation angular momentum plus the orbital angular momentum contributions from its moons produces  $L_T = 4.795 \times 10^{38} \text{ kg m}^2/\text{s}$  with a mass of  $M_T = 1.9 \times 10^{27} \text{ kg}$ . For Saturn and its moons,  $L_T = 7.109 \times 10^{37} \text{ kg m}^2/\text{s}$  for a mass  $M_T = 5.683 \times 10^{26} \text{ kg}$ . QCM predicts tangential velocities  $v_\phi$  for each co-axial concentric cylindrical equilibrium radius  $r_{eq}$  based upon the equation

$$v_\phi = \frac{m L_T}{r_{eq} M_T}. \quad (3)$$

Table 2: Radial equilibrium distances for Jupiter and Saturn

$m$	Jupiter $r_{eq}$ ( $10^7$ m)	Lat $\theta$	Saturn $r_{eq}$ ( $10^7$ m)	Lat $\theta$
1	1.73	75.98	2.00	70.53
2	2.45	69.97	2.82	61.97
3	3.00	65.19	3.46	54.78
4	3.46	61.02	4.00	48.19
5	3.87	57.20	4.47	41.84
6	4.24	53.60	4.90	35.25
7	4.58	50.14	5.29	28.16
8	4.90	46.75	5.66	19.38
9	5.19	43.39	6.00	0
10	5.47	40.00		
11	5.74	36.60		
12	6.00	32.95		
13	6.24	29.22		
14	6.48	25.00		
15	6.71	20.20		
16	6.93	14.25		
17	7.14	0		

Table 3: Radial equilibrium distances for Uranus and Neptune.

$m$	Uranus $r_{eq}$ ( $10^7$ m)	Lat $\theta$	Neptune $r_{eq}$ ( $10^7$ m)	Lat $\theta$
1	1.23	58.64	1.18	61.46
2	1.73	47.40	1.54	51.43
3	2.12	33.96	1.89	40.08
4	2.45	16.56	2.18	28.04
5			2.43	10.33

Thus, for the Jupiter  $m = 15$  and  $m = 16$  zones/bands at the  $20.20^\circ$  and  $14.25^\circ$  latitude flow regions, QCM predicts tangential velocities  $v_\phi$  of  $5.65 \times 10^4$  m/s and  $5.82 \times 10^4$  m/s, respectively. The zonal winds near the equatorial surface of Jupiter actually measure significantly lower values, having a maximum of about 100 m/s. Therefore, dynamic effects such as viscosity effects, etc., retard the flow in the atmosphere and are probably the cause of these much, much lower measured tangential velocity values than the predicted values.

For Saturn, for the  $m = 7$  and  $m = 8$  zones/bands at  $28.16^\circ$  and  $19.38^\circ$ , QCM predicts  $1.66 \times 10^4$  m/s and  $1.77 \times 10^4$  m/s tangential velocities, respectively. The data reveal much smaller flow velocities of about 300 m/s in these regions. Again, dynamic viscosity effects are probably reducing the predicted velocities to the measured velocities.

## 5 Conclusion

The zones/bands in the atmospheric flow regions on the surfaces of the Jovian planets appear to be in co-axial concen-

tric cylinders. These complex atmospheric flows possibly penetrate into the planetary bodies to depths of thousands of kilometers. Although a dynamical combination of Coriolis effects, temperature gradients, pressure gradients, magnetic field influences, etc., have been incorporated into existing dynamic models by several research groups, there has been no definitive single source proposed for the apparent cylindrical symmetries defining these flow regions.

Quantum celestial mechanics (QCM) has a gravitational wave equation (GWE) that we previously had applied in the Schwarzschild metric to predict rotating co-axial concentric cylindrical regions within all massive bodies. For one example, we applied the GWE inside the Earth to determine that the Antarctic Circumpolar Current (ACC), a water current traveling eastward about 2 meters/second faster than Earth's rotation rate at its latitude, could be explained by the application of the QCM quantization of angular momentum per unit mass equation

$$L/\mu = m L_T/M_T,$$

which relates an orbiting mass  $\mu$  of angular momentum  $L$  in orbit in a gravitationally bound system to the total mass  $M_T$  and total angular momentum  $L_T$ . When applied to all known orbiting planets in multi-planetary systems, we established that their planet orbital radii agree with this quantization of angular momentum per unit mass constraint equation.

Upon applying this angular momentum constraint equation to the four Jovian planets, we identified co-axial concentric rotating cylinders for zones/bands at reasonable radii, i.e. rotating cylindrical regions piercing the surfaces at numerous latitudes roughly agreeing with observational data for the zone/band locations as determined with observations by telescopes and spacecraft.

Therefore, we suggest that the true source of the co-axial concentric cylindrical flow regions in the Jovian planets has been identified to be the result of the QCM combination of Newtonian gravitational attraction and the repulsive effect of QCM quantization of angular momentum per unit mass. An improved understanding of the complex dynamics of these flow regions can now be achieved in the near future.

## Acknowledgements

The author appreciates the support of Sciencegems.com for the opportunity to investigate fundamental physics and its application to prevalent problems in Nature.

Received on June 25, 2025

## A Appendix: brief derivation of QCM equations

In 2003, Howard G. Preston and I introduced [6, 7] Quantum Celestial Mechanics (QCM), which is derived from the general relativistic Hamilton-Jacobi equation and a simple transformation that maintains the equivalence principle. The result was a new gravitational scalar wave equation (GWE) that, in

the Schwarzschild metric, predicts the quantization of angular momentum per unit mass. Here is an abbreviated derivation of the equations to be used for analyzing the Jovian planets.

From the general relativistic Hamilton-Jacobi equation,

$$g^{\alpha\beta} \frac{\partial S}{\partial x^\alpha} \frac{\partial S}{\partial x^\beta} - \mu^2 c^2 = 0, \quad (4)$$

the transformation

$$\Psi = e^{iS'/\mu c H} \quad (5)$$

introduces a wave function  $\Psi$ , with  $S$  the action,  $\mu$  the mass of the orbiting object, and  $S' = S/\mu c$  so that the equivalence principle is obeyed. For a detailed derivation showing all the mathematical steps, see [6].

We defined a system scale length  $H$  by

$$H = \frac{L_T}{M_T c} \quad (6)$$

for the total gravitationally bound system mass  $M_T$  having total angular momentum  $L_T$  and  $c$  being the speed of light in vacuum.

Following through with the mathematical steps produced a scalar gravitational wave equation (GWE)

$$g^{\alpha\beta} \frac{\partial^2 \Psi}{\partial x^\alpha \partial x^\beta} + \frac{\Psi}{H^2} = 0. \quad (7)$$

Expressing the GWE in the Schwarzschild metric, a separation of variables leads to differential equations in coordinates  $(t, r, \theta, \phi)$  that produce quantization conditions.

The angular parts dictate the quantization of angular momentum *per unit mass* for orbital angular momentum  $L$  as

$$\frac{L}{\mu} = m c H \quad (8)$$

for integer  $m$ . The radial equation leads to the quantization of energy *per unit mass* equation

$$E_n = -\mu c^2 \frac{r_s^2}{8n^2 H^2} \quad (9)$$

for integer  $n$ .

The expected value of the QCM orbital radial acceleration near the orbital equilibrium radius is defined by

$$\ddot{r}_{eq} = -\frac{GM}{r^2} + \frac{\ell(\ell+1)L_T^2}{r^3 M_T^2}. \quad (10)$$

For cylindrical coordinates, the  $\ell(\ell+1)$  is replaced by  $m^2$ .

For comparison, recall that the standard Newtonian gravitation has

$$\ddot{r}_{eq} = -\frac{GM}{r^2} + \frac{L^2}{\mu^2 r^3} \quad (11)$$

and, because the angular momentum  $L = \mu \sqrt{GM} r$  and the angular velocity  $\dot{\phi} = L/\mu r^2$  for a circular orbit, then  $\ddot{r} = 0$  and the radial acceleration per mass  $(\ddot{r} - r\dot{\phi}^2)$  equals  $-GM/r^2$ .

Consequently, QCM has both the Newtonian attraction term and a repulsive angular momentum term around each equilibrium orbital radius, which results in the prediction of allowed orbital radii that are a sparse subset of the Newtonian ones. In addition, there will be equilibrium radii within planets at which a QCM acceleration occurs.

## References

1. Fletcher L. N., Kaspi Y., Guillet T., Showman A. P. How well do we understand the belt/zonal circulation of Giant Planet atmospheres? *Space Sci Rev*, 2020, v. B216, 30. arXiv:1907.01822v2.
2. Kaspi Y., Galanti E., *et al.* Observational evidence for cylindrically oriented zonal flows on Jupiter. *Nature Astronomy*, 2023, v. 7, 1463–1472.
3. Chachan Y. and Stevenson D. J. A Linear Approximation for the Effect of Cylindrical Differential Rotation on Gravitational Moments: Application to the Non-Unique Interpretation of Saturn's Gravity. *Icarus*, 2019, v. 323, 87–98. arXiv: 1902.10728v1.
4. Duer K., Galanti E., Kaspi Y. Gas Giant Simulations of Eddy-Driven Jets Accompanied by Deep Meridional Circulation. *AGU Advances*, 2023, v. 4, 32023AV000908. arXiv: astro-ph/2312.10651.
5. Helled R. and Howard S. Giant planet interiors and atmospheres. arXiv: astro-ph/2407.05853.
6. Preston H. G. and Potter F. Exploring Large-scale Gravitational Quantization without  $\hbar$  in Planetary Systems, Galaxies, and the Universe. arXiv: gr-qc/0303112.
7. Potter F. and Preston H. G. Quantum Celestial Mechanics: large-scale gravitational quantization states in galaxies and the Universe. In: 1st Crisis in Cosmology Conference: CCC-I, Lerner E. J. and Almeida J. B., eds., AIP CP822, 2006, 239–252.
8. Potter F. Predicting Total Angular Momentum in TRAPPIST-1 and Many Other Multi-Planetary Systems Using Quantum Celestial Mechanics. *Prog. in Physics*, 2018, v. 14 (3), 115–120.
9. Potter F. Galaxy Clusters: Quantum Celestial Mechanics (QCM) Rescues MOND? *Prog. in Physics*, 2024, v. 20 (2), 100–102.
10. Potter F. and Preston H. G. Cosmological Redshift Interpreted as Gravitational Redshift. *Prog. in Physics*, 2007, v. 3 (2), 31–33.
11. Potter F. Antarctic Circumpolar Current: Driven by Gravitational Forces? *Prog. in Physics*, 2021, v. 17 (1), 99–103.
12. Ma X. and Tkačič H. Seismic low-velocity equatorial torus in the Earth's outer core: Evidence from the late-coda correlation wavefield. *Science Advances*, 2024, v. 10 (35).